

Synthesis, Physicochemical Properties, and Biological Evaluation of Hydroxypyranones and Hydroxypyridinones: Novel Bidentate Ligands for Cell-Labeling

Beverley L. Ellis,^{*,†} Anne K. Duhme,[†] Robert C. Hider,[†] M. Bilayet Hossain,[‡] Safia Rizvi,[‡] and Dick van der Helm[‡]

Department of Pharmacy, King's College London, Manresa Road, London SW3 6LX, U.K., and Department of Chemistry, Oklahoma University, 620 Parrington Oval, Norman, Oklahoma 73019-0370

Received March 18, 1996[®]

The synthesis of a range of hydroxypyranones and hydroxypyridinones with potential for the chelation of indium(III) is described. The crystal structures of two of the indium complexes are presented. The distribution coefficients of the ligands and the corresponding iron(III), gallium(III), and indium(III) complexes are reported. Good linear relationships between the distribution coefficients of the iron and gallium complexes and iron and indium complexes were obtained. In contrast a nonlinear relationship was obtained between the distribution coefficient of the free ligand and the distribution coefficient of the three groups of complexes. This latter relationship was used to identify compounds with optimal cell labeling properties. Two such compounds both 6-(alkoxymethyl)-3-hydroxy-4*H*-pyran-4-ones have been compared with tropolone for their ability to label human leucocytes with ¹¹¹In. The leucocyte labeling efficiencies of the selected ligands were greater and the *in-vitro* plasma stabilities were similar to that of ¹¹¹In-tropolonate. These results suggest that the new bidentate ligands may offer advantages over those currently used for cell-labeling.

Introduction

The radiolabeling of leucocytes with ¹¹¹In to facilitate clinical investigations is well-established. A requisite for such studies is that the radiolabeled cells follow their natural behavior when reinjected and are not damaged as a result of the labeling technique or toxicity of the ligand or radionuclide.¹ Ionic indium will not penetrate cell membranes and is susceptible toward hydrolysis at pH values above 3.5. In contrast, when indium is coordinated by bidentate ligands to form neutral 3:1 complexes, it is protected against hydrolysis and can permeate cell membranes, allowing the radionuclide to become firmly attached to the cytoplasmic components on subsequent dissociation of the complex. Oxine (8-hydroxyquinoline) **1** was the first agent used to label mixed cell populations;^{2,3} however, this agent will not label cells satisfactorily in the presence of plasma. Tropolone (2-hydroxy-2,4,6-cycloheptatrienone) (**2**) was introduced as an alternative in 1981⁴ by virtue of its ability to label cells in the presence of plasma^{5,6} and is widely used in the United Kingdom. Merc (2-mercaptopyridine *N*-oxide) (**3**) was also introduced as an alternative to tropolone,^{7,8} but has not been as widely used in a clinical setting. Both oxine and tropolone have been reported to be toxic to cells, particularly lymphocytes.^{9–12}

3-Hydroxypyridinones and 3-hydroxypyranones bind trivalent cations including indium in a similar manner to that of oxine.¹³ These chelators bind indium to form neutral 3:1 complexes and their hydrophobicity may be adjusted by alkyl substitution. The gallium and indium complexes of a limited range of 3-hydroxypyridin-4-ones

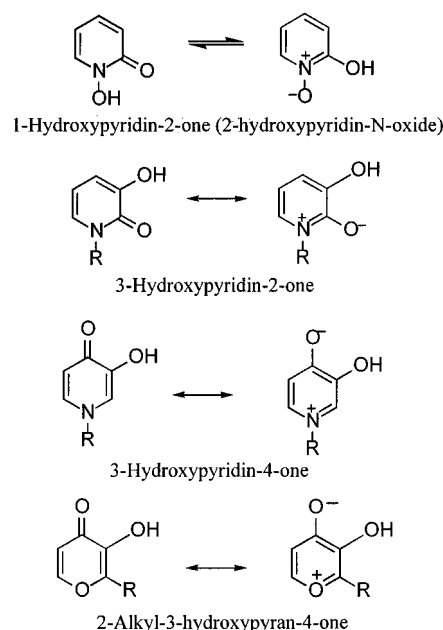


Figure 1. The mesomeric forms of hydroxypyridinones and hydroxypyranones.

and 3-hydroxypyran-4-ones have been previously characterized.^{14–16} The hydroxypyridinones may be divided into three classes: these are the 1-hydroxypyridin-2-ones, 3-hydroxypyridin-2-ones, and 3-hydroxypyridin-4-ones (Figure 1). Only the 1-hydroxypyridin-2-ones exist in tautomeric equilibrium; both tautomers on deprotonation produce the same anion. The other two pyridinone classes only have one tautomer; the benzoid mesomer makes a significant contribution which results in a high charge density on the carbonyl oxygen thus endowing compounds with good metal-chelating properties. A similar situation occurs with the 3-hydroxypyranones. The 1-hydroxypyridin-2-ones are negatively charged at physiological pH and are therefore not ideal

* Address for correspondence: Dr. Beverley Ellis, Department of Nuclear Medicine, Manchester Royal Infirmary, Oxford Rd., Manchester M13 9WL, U.K.

[†] King's College London.

[‡] Oklahoma University.

[®] Abstract published in *Advance ACS Abstracts*, August 1, 1996.

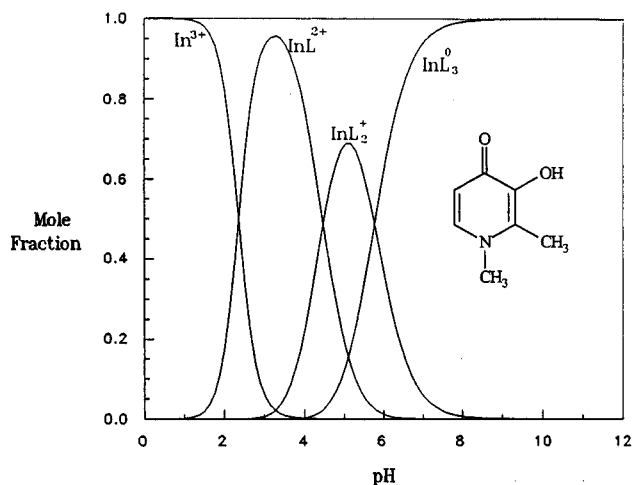


Figure 2. Speciation plot of 1,2-dimethyl-3-hydroxy-4(1*H*)-pyridin-4-one and indium(III). Concentration of pyridinone 10^{-5} M, concentration of indium(III) 10^{-6} M. The following parameters¹⁶ were incorporated into the model for the system. $\log K_1 ML = 13.60$; $\log K_2 ML_2 = 23.90$; $\log K_3 ML_3 = 32.90$; $pK_{a1} = 9.65$; $pK_{a2} = 13.28$. InL^{2+} , InL_2^+ , and InL_3^0 are the 1:1, 1:2, and 1:3 indium pyridinone complexes, respectively.

cell-labeling agents. In contrast both the 3-hydroxypyridin-2-ones and 3-hydroxypyridin-4-ones are uncharged and bind In^{3+} to form neutral 3:1 complexes at pH 7.4, and this species dominates over the pH range 6–10 (Figure 2). The hydroxypyranones (Figure 1) also form neutral 3:1 complexes with indium at pH 7.4, and this species dominates over the pH range 6–10; indeed the speciation plot for indium 2-ethyl-3-hydroxypyran-4-one (ethylmaltol) is similar to that in Figure 2. Both the hydroxypyridinones and hydroxypyranones are of relatively low toxicity.^{13,17–19} The hydroxypyranone 3-hydroxy-2-methylpyran-4-one (maltol), for instance has an LD_{50} value in the rat of 1444 mg/kg. The low toxicities may be partially a consequence of rapid metabolism.^{18–20} As such compounds are predicted to have the advantage of lower toxicity when compared to the current cell-labeling agents, we have synthesized a range of hydroxypyridinone and hydroxypyranone analogues. The hydrophobicity of these compounds can be adjusted systematically by alkyl substitution in order to control the diffusion of the metal complex through biological membranes.

The distribution coefficient values for the free ligand and for the Fe, Ga, and In complexes for each bidentate ligand together with those of the currently used cell-labeling agents are reported. Cell-labeling studies associated with selected bidentate chelators are reported.

Chemistry

3-Hydroxy-4*H*-pyran-4-one. The synthesis of 3-hydroxy-4*H*-pyran-4-one (5) (Scheme 1) adopted in this study was found to be superior to the method of Tate and Miller.²¹ This method involves the protection of kojic acid; the subsequent oxidation of the resulting benzylkojic acid to benzylcomenic acid is achieved using Jones reagent.^{22,23} Decarboxylation was accomplished by refluxing benzylcomenic acid in 1-methyl-2-pyrrolidinone. Deprotection of the 3-hydroxyl group to afford 3-hydroxy-4*H*-pyran-4-one was achieved using 4 M hydrochloric acid.

3-Hydroxy-2-methyl-4*H*-pyran-4-one (6) (maltol) and

2-ethyl-3-hydroxy-4*H*-pyran-4-one (7) (ethylmaltol) were commercially available (Pfizers Ltd., Kent, U.K.).

6-(Alkoxyethyl)-3-hydroxy-4*H*-pyran-4-ones. Reaction of benzylkojic acid with alkyl halides and sodium hydride in dry *N,N*-dimethylformamide resulted in the production of the benzylated alkoxyethyl derivatives **8–11** (Scheme 1). Removal of the protecting benzyl group (4 M HCl) yielded the pyranones **12–15** (Table 1).

2-Alkyl-3-hydroxy-6-methyl-4*H*-pyran-4-ones. A method similar to that described by Campbell et al.²⁴ was adopted for the synthesis of 3-hydroxy-6-methyl-4*H*-pyran-4-one (**16**) (allomaltol) (Scheme 2). Reduction of chlorokojic acid with zinc dust and concentrated hydrochloric acid resulted in the production of 3-hydroxy-6-methyl-4*H*-pyran-4-one (**16**). Subsequent condensation with aldehydes resulted in the corresponding 2-(1-hydroxyalkyl)-3-hydroxy-6-methyl-4*H*-pyran-4-ones **17–20**. Reduction of the latter with zinc dust and concentrated hydrochloric acid resulted in the formation of 2-alkyl-3-hydroxy-6-methyl-4*H*-pyran-4-ones **21–24** (Table 1).

1-Alkyl-3-hydroxy-2*H*-pyridin-2-ones. The *N*-alkylated-3-methoxy-2*H*-pyridin-2-ones were synthesized by utilising a method similar to that reported by Rogers et al.²⁵ (Scheme 3). The commercially available 3-methoxy-2(1*H*)-pyridin-2-one was allowed to react with an alkyl halide and potassium hydroxide in the corresponding alcohol. The 3-methoxy group was cleanly cleaved using boron tribromide²⁶ resulting in the 1-alkyl-3-hydroxy-2*H*-pyridin-2-ones **29–32** (Table 2).

1,2-Substituted 3-Hydroxy-4*H*-pyridin-4-ones. The 1,2-substituted 3-hydroxy-4*H*-pyridin-4-ones (Table 2) were synthesized by the method of Harris and co-workers²⁷ as modified by Dobbin et al.²⁸ The synthesis of 1-(2-aminoethyl)-3-hydroxy-4*H*-pyridin-4-one (**36**) was achieved using the method of Hare et al.²³

Determination of Distribution Coefficients

The distribution coefficients of the chelators were determined using a buffered octanol/aqueous system. A modified automated continuous flow technique^{29,30} was chosen in preference to the traditional shake-flask method³¹ owing to a greater accuracy and reproducibility of measurements. The filter probe method was, however, unsuitable for determining the distribution coefficients of the In(III) and Ga(III) complexes of the bidentate ligands, owing to poor spectral discrimination between the free ligand and complexes. Spectroscopic and radiometric analyses were used to measure the distribution coefficients of the iron(III) complexes. A good agreement between the two methods was obtained. The radiometric method was subsequently adopted for the In and Ga complexes using ¹¹¹In and ⁶⁷Ga, respectively.

Biological Experiments

The effect of ligand concentration on the uptake of the ¹¹¹In-complexes of **14** and **15** into erythrocytes was measured. The labeling efficiencies and *in-vitro* plasma stabilities of the ¹¹¹In-complexes of **14**, **15**, and **2** using "mixed" leucocytes were determined.

Results

Distribution Coefficients. Free Ligands. The distribution coefficients between octanol and aqueous

Scheme 1

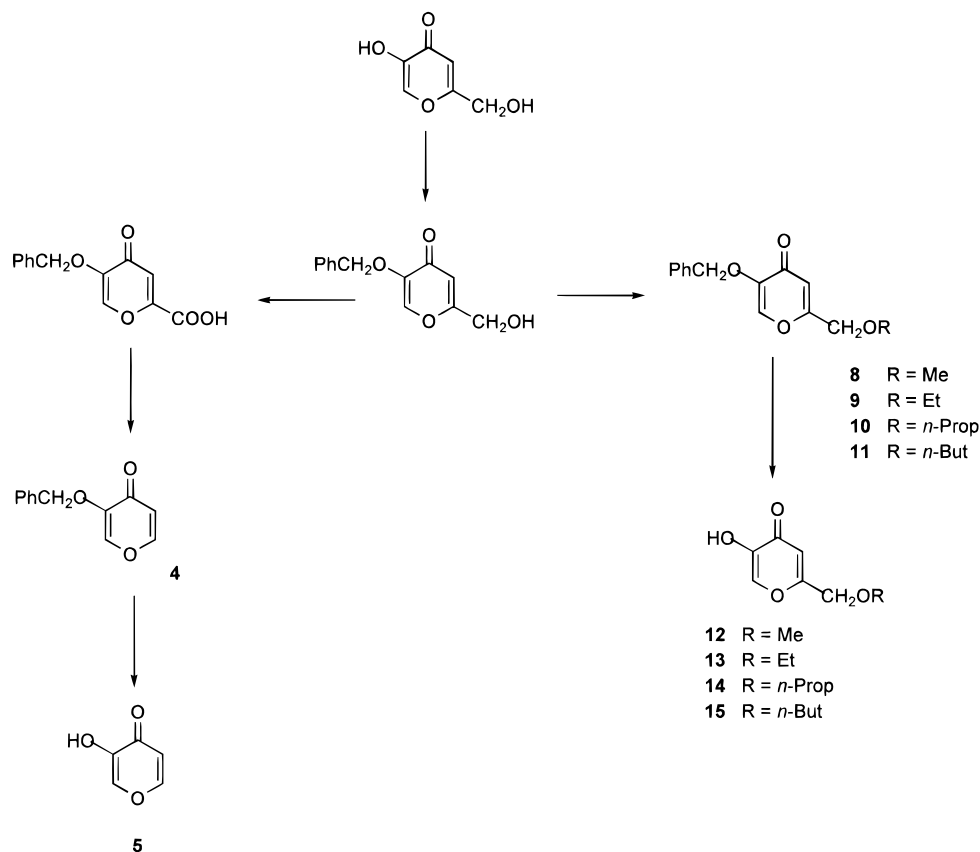


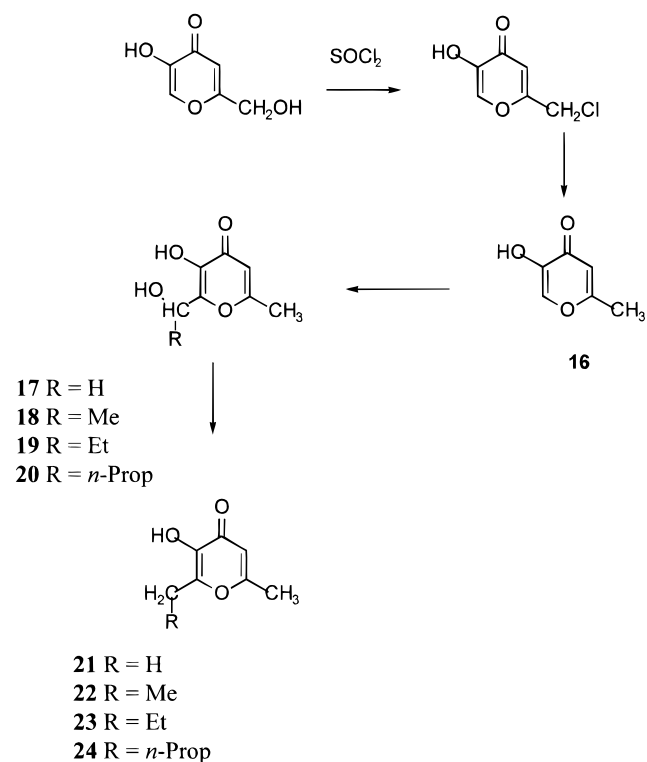
Table 1

compd	R	R'	X
4	H	H	Bz
5	H	H	H
6	H	Me	H
7	H	Et	H
8	CH ₂ OMe	H	Bz
9	CH ₂ OEt	H	Bz
10	CH ₂ <i>O</i> <i>n</i> -Pr	H	Bz
11	CH ₂ <i>O</i> <i>n</i> -Bu	H	Bz
12	CH ₂ OMe	H	H
13	CH ₂ OEt	H	H
14	CH ₂ <i>O</i> <i>n</i> -Pr	H	H
15	CH ₂ <i>O</i> <i>n</i> -Bu	H	H
16	Me	H	H
17	Me	CH ₂ OH	H
18	Me	CH(Me)OH	H
19	Me	CH(Et)OH	H
20	Me	CH(<i>n</i> -Pr)OH	H
21	Me	Me	H
22	Me	Et	H
23	Me	<i>n</i> -Pr	H
24	Me	<i>n</i> -Bu	H

phase buffered at pH 7.4 are presented in Table 3. On ascending a homologous series of compounds, the increase in hydrophobicity is reflected by a rise in distribution coefficient.

Metal Complexes. The values of the distribution coefficients for the metal complexes between buffered aqueous phase (pH 7.4) and octanol are shown in Table 3. The expected increase in distribution coefficient upon elongation of the alkyl chain was observed for all the metal complexes. In general the value obtained for the

Scheme 2



metal complex is greater than that of the corresponding ligand. This is to be expected as the complex presents a more extended hydrophobic surface to its environment.

Graphs plotted of the log *D* values of each metal complex of the chelators against the log *D* values of the

Scheme 3

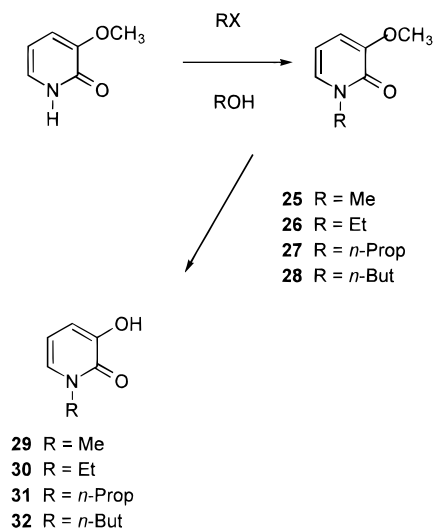


Table 2

compd	R	R'	compd	R	R'
25	Me	Me	33	<i>n</i> -Bu	Me
26	Et	Me	34	<i>n</i> -pentyl	Me
27	<i>n</i> -Pr	Me	35	<i>n</i> -hexyl	Me
28	<i>n</i> -Bu	Me	36	CH ₂ CH ₂ NH ₂	H
29	Me	H			
30	Et	H			
31	<i>n</i> -Pr	H			
32	<i>n</i> -Bu	H			

corresponding free ligand are shown in Figure 3. A cursory inspection indicates a broad linear relationship. However the dispersion of data about the linear regression line is wide; for instance, for iron(III) the correlation coefficient is only 0.8. There are many appreciable deviations from the linear relationship, for example the value for the log *D* of iron-tropolonate as determined from the regression equation is 0.02, whereas the experimentally determined value is 1.74. Therefore the usefulness of the linear regression equation as a means for predicting the *D* value of a complex from the *D* value of the free ligand is low. The standard deviations of the data are sufficiently small (Table 3) that it may be assumed that the deviations of the data points from the regression line are genuine. Thus the oscillations of the data are real and probably reflect structural aspects of the ligands. This is confirmed by similar patterns obtained with iron, gallium, and indium complexes; indeed the similarities are particularly striking, with the only appreciable difference being with the hydrophilic complexes where the trend deviates slightly. It is not surprising that the gallium and iron complexes have similar profiles as the radii of the two ions are almost equal.¹³ Figure 4 illustrates the excellent linear relationship between the log *D* values of the iron complexes and the log *D* values of the corresponding gallium complexes. The correlation coefficient is 0.99, and the slope is close to 1. A similar relationship holds for indium; however, a slightly greater spread of data is indicated by the correlation coefficient of 0.95. On average the data for the log *D* values for the indium

complexes are slightly greater than those of gallium. The trend is more pronounced for the hydrophilic complexes.

It is important to record the chemical nature of the compounds at the peaks of the relationship in Figure 3 i.e. **2**, **13**, **14**, **15**, **32** and **34** and at the troughs of the same relationship i.e. **6**, **7**, **21**, **22**, **29** and **30**. Compounds **13**, **14**, and **15** all have substituent alkoxy groups in the 6-position which are effectively para to the chelating group, thus making the molecule more extended from the site of chelation. This possibly allows greater interaction with the solvent molecules and concomitantly a higher *D* value for a given molecular mass. In contrast compounds **6**, **7**, **21**, **22**, **29**, and **30** each have an alkyl substituent ortho to the chelating group, making the complex more compact, thus offering the possibility of less interaction with the solvent molecules.

X-ray Crystallography. The ORTEP plots of the X-ray structures of the indium(III) complexes of ligands **7** and **14** (**37** and **38**) are shown in Figures 5 and 6, respectively. The reason for choosing the complexes **37** and **38** for crystal structure analysis is that they represent the classes of compounds found at the troughs and peaks of the relationship shown in Figure 3. In both the complexes the indium atom has octahedral geometry with all the hydroxo oxygen atoms bound in *trans* position to the keto oxygens (*fac* configuration). The octahedron is more distorted in **37** than in **38** as reflected by the axial O–M–O angles, [156.1(1)°, 152.2(1)°, and 157.7(1)°] in complex **37** and [163.4(3)°, 162.7(3)°, and 160.1(3)°] in complex **38**, and also by their twist angles, 30.1(1)° in **37** and 39.7(4)° in **38**. This is possibly due to the *ortho* substitution in **7** compared to *para* in **14**. The chelate angle in the two In complexes is closely similar (77°) and it seems to be a characteristic for the indium ion.

The observed *fac* configuration is the one favored by the *trans* influence, because all strong donor atoms are coordinated in *trans* position to the weaker donor atoms. Consequently, there is a significant difference between the In–O(hydroxo) and In–O(keto) distances, 0.07 Å in **37** and 0.08 Å in **38** (Table 4). The particularly large difference in these complexes is most likely due to the special electronic features of the hydroxypyridone ligand, as the corresponding differences in hydroxypyridin-4-one or hydroxamate are much smaller: 0.03 Å in tris(3-hydroxy-4-pyridinone)indium³² and 0.02 Å for tris(benzohydroxamato)indium.³³ Accordingly, a quite large difference of 0.055 Å, has been observed for tris-(maltol)aluminum,³⁴ although in this complex the coordination geometry is *meridional*.

A comparison of the average bond distances of the pyranone skeleton in the complexes **37** and **38** with those observed for the ligands (**7**³⁵) and (**14**)³⁶ (Table 4) show that the changes in the bond distances in the pyran ring are small.

Effect of Ligand Concentration on Erythrocyte Labeling. Compounds **14** and **15** were selected for cell-labeling studies. The reason for choosing these compounds is that they had a high distribution coefficient for the ¹¹¹In complex and a relatively low distribution coefficient for the uncomplexed ligand. This would enable the ¹¹¹In complex to be delivered into the cell and minimize accumulation of the free ligand in the

Table 3. Distribution Coefficient Values of Bidentate Chelators and Corresponding Metal Complexes^c

compd	mean log <i>D</i> free ligand	mean log <i>D</i> iron(III) complex	mean log <i>D</i> gallium(III) complex	mean log <i>D</i> indium(III) complex	methods ^d
1	1.87 ± 0.02 (<i>n</i> = 9)	3.02 ± 0.04 ^a	3.12 ± 0.004 ^a	3.07 ± 0.07 ^b	A, C
2	-0.14 ± 0.02 (<i>n</i> = 4)	1.74 ± 0.03 ^b	1.58 ± 0.01 ^b	1.94 ± 0.03 ^b	A, C
5	-0.92 ± 0.04 (<i>n</i> = 7)	-2.00 ± 0.03	-1.48 ± 0.07	-1.18 ± 0.07	A, B
6	0.05 ± 0.001 (<i>n</i> = 7)	-0.59 ± 0.03	-0.81 ± 0.10	-0.09 ± 0.01	A, B
7	0.63 ± 0.007 (<i>n</i> = 7)	0.72 ± 0.03	0.59 ± 0.02	1.33 ± 0.05	A, B
12	-0.62 ± 0.08 (<i>n</i> = 12)	-0.97 ± 0.12	-0.87 ± 0.04	-0.50 ± 0.03	A, B
13	-0.38 ± 0.06 (<i>n</i> = 5)	0.53 ± 0.05	0.28 ± 0.02	0.95 ± 0.05	A, B
14	0.30 ± 0.04 (<i>n</i> = 10)	2.22 ± 0.04	2.22 ± 0.02	2.53 ± 0.01	A, C
15	0.78 ± 0.03 (<i>n</i> = 10)	2.64 ± 0.02 ^a	2.54 ± 0.01 ^a	2.69 ± 0.06 ^a	A, C
16	-0.59 ± 0.02 (<i>n</i> = 5)	-0.72 ± 0.11	-0.74 ± 0.01	-0.19 ± 0.02	A, B
21	0.44 ± 0.005 (<i>n</i> = 5)	0.39 ± 0.01	0.16 ± 0.05	0.70 ± 0.01	A, B
22	1.07 ± 0.02 (<i>n</i> = 5)	1.57 ± 0.02	1.36 ± 0.00	2.13 ± 0.02	A, C
23	1.40 ± 0.01 (<i>n</i> = 4)	2.57 ± 0.05 ^a	2.55 ± 0.003 ^a	2.09 ± 0.07 ^b	A, C
24	1.92 ± 0.07 (<i>n</i> = 5)	3.06 ± 0.05 ^a	3.06 ± 0.09 ^a	2.25 ± 0.05 ^b	A, C
29	-0.28 ± 0.004 (<i>n</i> = 5)	-1.02 ± 0.03	-1.14 ± 0.09	-0.41 ± 0.01	A, B
30	0.20 ± 0.001 (<i>n</i> = 5)	0.10 ± 0.02	-0.04 ± 0.01	0.76 ± 0.01	A, B
31	0.69 ± 0.01 (<i>n</i> = 9)	1.49 ± 0.04	1.25 ± 0.02	2.11 ± 0.02	A, C
32	1.18 ± 0.003 (<i>n</i> = 6)	2.64 ± 0.01 ^a	2.63 ± 0.01	3.20 ± 0.01 ^b	A, C
33	0.71 ± 0.005 (<i>n</i> = 11)	1.36 ± 0.02	1.24 ± 0.04	1.76 ± 0.01	A, C
34	1.24 ± 0.006 (<i>n</i> = 24)	2.97 ± 0.004	2.84 ± 0.10	3.08 ± 0.03 ^b	A, C
35	1.90 ± 0.03 (<i>n</i> = 6)	3.47 ± 0.07 ^a	3.40 ± 0.16 ^a	3.20 ± 0.04 ^b	A, C
36	-0.66 ± 0.09 (<i>n</i> = 5)	-1.34 ± 0.10	-1.80 ± 0.17	-1.54 ± 0.15	A, B

^a Ligand:metal concentration 1×10^{-4} M: 1×10^{-5} M. ^b Ligand:metal concentration 1×10^{-5} M: 1×10^{-6} M. ^c *n* = 3 for all metal complex distribution coefficient determinations. Ligand:metal concentration 1×10^{-3} M: 1×10^{-4} M unless specified. ^d Method A: Free ligand *D* value determination using filter probe technique. Method B: Radiometric method for complexes with *D* values <10. Method C: Radiometric method for complexes with *D* values >10.

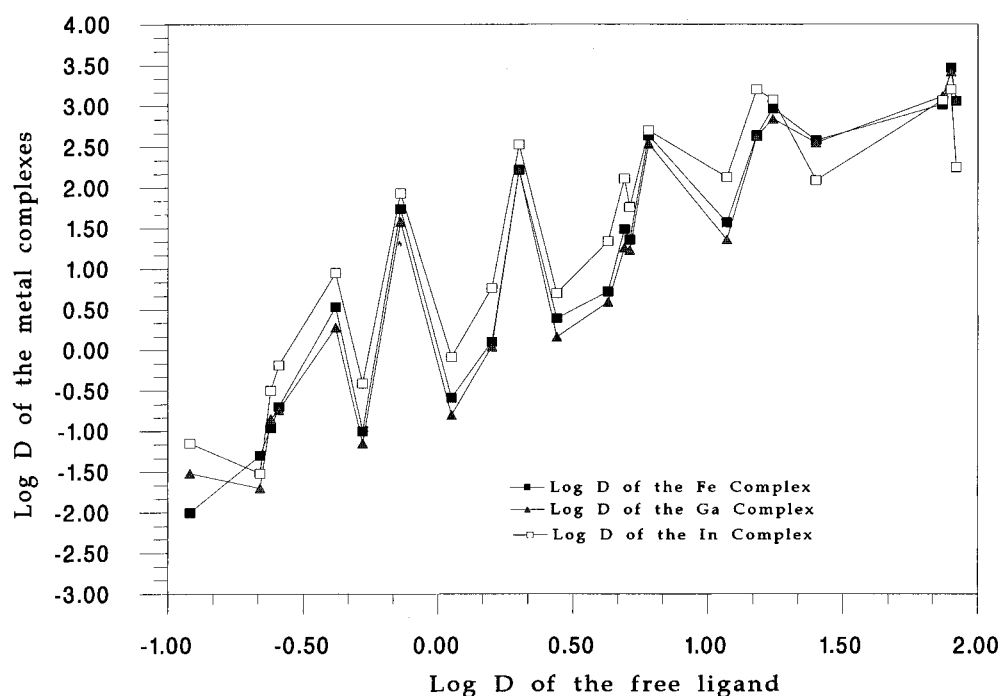


Figure 3. Plot of the log distribution coefficient values (*log D*) of the metal complexes versus the *log D* values of the corresponding free ligand. Distribution coefficients were determined using MOPS buffer (20 mM, pH 7.4)/octanol systems.

membrane, and therefore such compounds are predicted to be less toxic than the current cell-labeling agents. Human erythrocytes were incubated with the ¹¹¹In complexes of the hydroxypyranones **14** and **15** at varying ligand concentrations. The effect of ligand concentration on the labeling efficiencies of the above ¹¹¹In complexes is shown in Figure 7. At ligand concentrations below 1×10^{-5} M, the labeling efficiencies decrease rapidly below 50%. With increasing ligand concentration, the labeling efficiencies rise to approximately 90% by 2×10^{-4} M. Further increases in ligand concentration to 1×10^{-3} M produce only marginal increases in labeling efficiency. Both compounds follow similar trends; however, below ligand concentrations of 2×10^{-4}

M, markedly higher labeling values are observed with the ¹¹¹In complex of **15**.

Leucocyte Labeling and *in-Vitro* Plasma Stabilities. "Mixed" leucocytes were incubated with the ¹¹¹In complexes of **14**, **15**, and **2**. The leucocyte labeling efficiencies are presented in Table 5. The labeling efficiencies for the ¹¹¹In complexes of **14** and **15** are appreciably greater than that of ¹¹¹In-tropolonate. The total percentage of ¹¹¹In released per hour from the "mixed" leucocytes labeled with the ¹¹¹In-complexes of **14**, **15**, and **2** are shown in Figure 8. Similar trends are observed for all three complexes. Generally the amount of ¹¹¹In released in the first hour was greater than that released in subsequent hours.

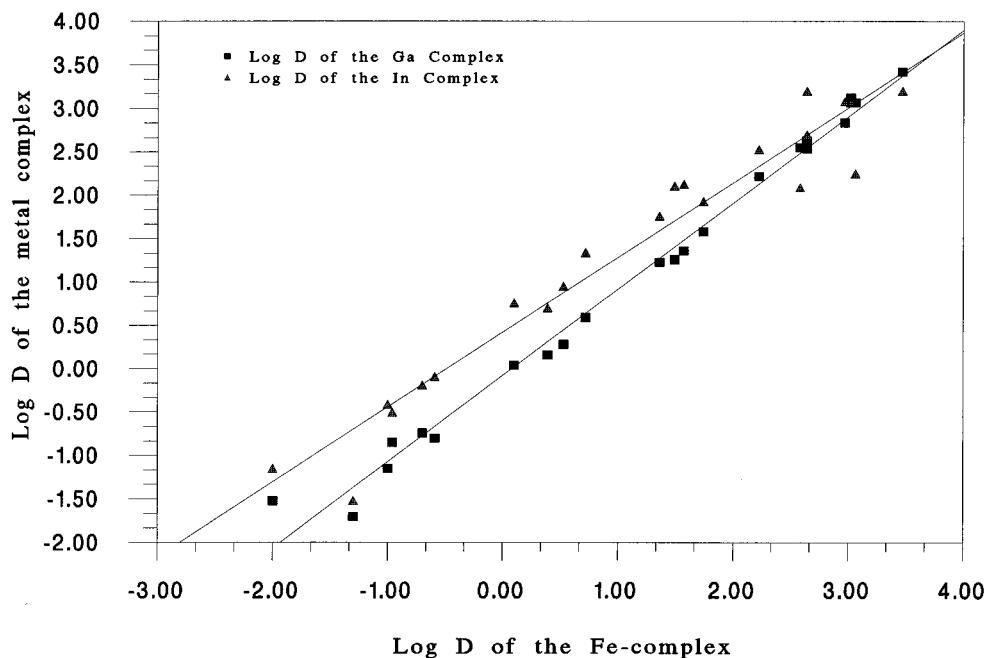


Figure 4. Plot of the log D values of the Ga and In complexes versus the log D values of the iron(III) complexes of the bidentate ligands. (Log D of the In complex) = $0.422 + 0.862$ (log D of the Fe(III) complex), correlation coefficient $r = 0.945$; (log D of the Ga complex) = $-0.077 + 0.995$ (log D of the Fe(III) complex), correlation coefficient $r = 0.989$. The mean of three independent measurements is shown.

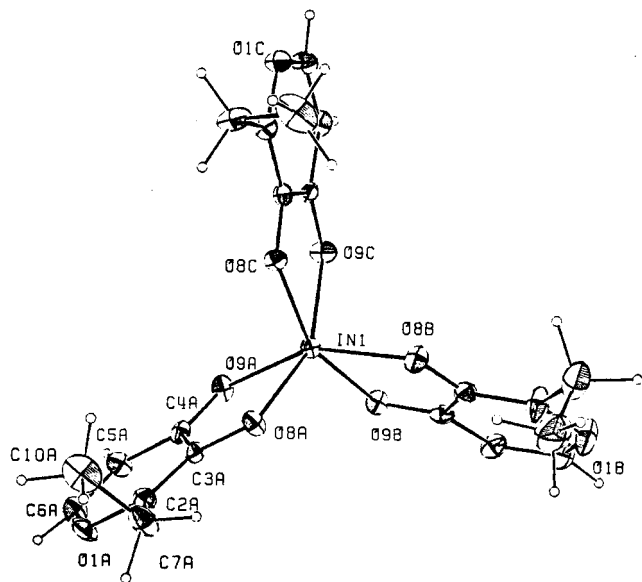


Figure 5. Perspective view of indium complex **37** showing the displacement ellipsoids at the 30% probability level.

Discussion

Eighteen bidentate ligands have been synthesized covering a wide range of distribution coefficients. All the ligands bind tribasic cations tightly ($\beta_3 \approx 10^{30} \text{ M}^{-1}$) to form neutral 3:1 complexes over the pH range 5.0–8.0 (Figure 2). The relationship between the ligand D values and the complex D values is complicated (Figure 3), but conserved for the three metals investigated, namely iron(III), gallium(III), and indium(III). Indeed despite this complicated relationship, there is an excellent linear correlation between the log D values of the three metal complexes (Figure 4). Significantly there is a regular increase in the log D values with increasing alkyl group size in each series of compounds (Table 6).

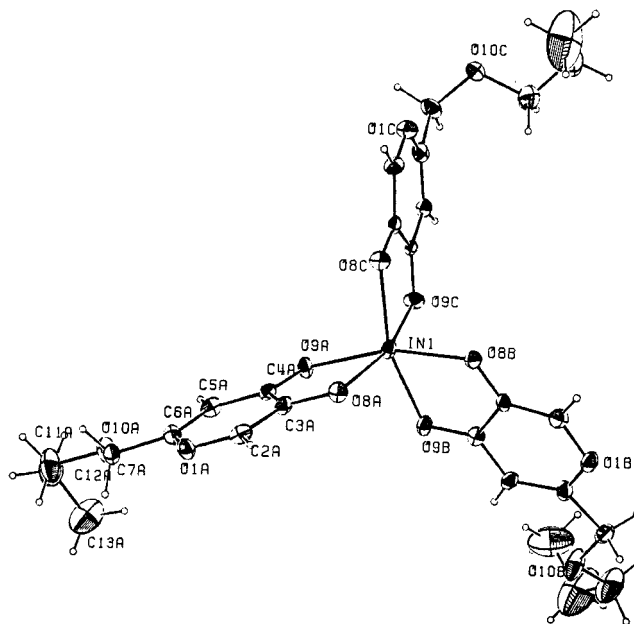


Figure 6. Perspective view of indium complex **38** showing the displacement ellipsoids at the 30% probability level.

Table 4. Comparison of the Average Bond Distances (Å) in the Free Hydroxypyranone Ligands and Indium Complexes of **7** and **14** and the Corresponding Complexes **37** and **38**

bond	7 ³⁵	14 ³⁶	37	38
O(1)–C(2)	1.366(2)	1.363(4)	1.373(8)	1.35(1)
O(1)–C(6)	1.344(2)	1.345(4)	1.345(9)	1.33(9)
C(2)–C(3)	1.358(3)	1.348(4)	1.369(9)	1.36(1)
C(3)–C(4)	1.443(3)	1.440(4)	1.442(8)	1.46(1)
C(4)–C(5)	1.438(3)	1.425(5)	1.422(9)	1.42(1)
C(5)–C(6)	1.341(3)	1.325(5)	1.338(10)	1.35(1)
C(3)–O(h)	1.354(2)	1.351(4)	1.322(7)	1.30(1)
C(4)–O(k)	1.248(2)	1.244(4)	1.279(7)	1.26(1)

The π value (corresponding to the $\Delta \log D$ effect of a substituent) derived by Hansch³⁷ for a $-\text{CH}_2-$ or CH_3 group is 0.5.

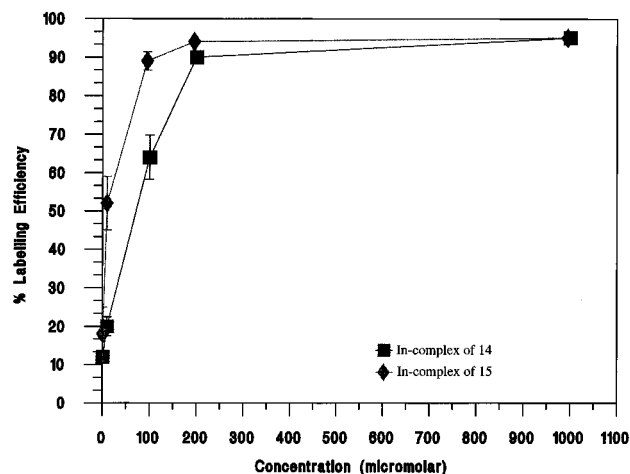


Figure 7. The effect of ligand concentration on the uptake of the ^{111}In complexes of **14** and **15** by erythrocytes. Human erythrocytes were incubated with varying concentrations of the ^{111}In complexes for 15 min and the labeling efficiencies determined. The mean of three independent determinations is shown with the standard error.

Table 5. Labeling Efficiencies of ^{111}In Complexes of **14**, **15**, and **2** with "Mixed" Leucocytes

^{111}In complex	% labeling efficiency ^a
14	89 ± 3.4
15	87 ± 4.2
2	76 ± 5.0

^a Mean of 3 ± SD.

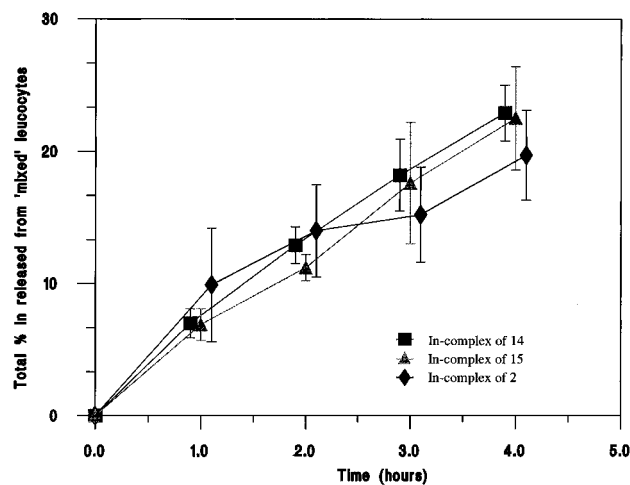


Figure 8. The release of ^{111}In from "mixed" leucocytes labeled with the ^{111}In complexes of **14**, **15**, and **2** against time. "Mixed" leucocytes labeled with the ^{111}In complexes were incubated with 3 mL of cell-free plasma, respectively, for 1 h, and the % ^{111}In released was determined. The process was repeated for 2, 3, and 4 h. The mean of three independent readings is shown with the standard error.

Analysis of the oscillating relationship between $\log D$ values of the free ligand and metal complexes shows that compounds **2**, **13**, **14**, **15**, **32** and **34** possess relatively high D complex/ D ligand ratios whereas for compounds **6**, **7**, **21**, **22**, **29**, and **30** the ratio is relatively low. Those compounds possessing a high ratio have, with the exception of tropolone **2**, side chains containing more than three atoms in length. In contrast, compounds with a low ratio possess side chains that without exception are restricted to only one or two carbon atoms in length.

Table 6. $\Delta \log D$ Values for 3-Hydroxypyranones and 3-Hydroxypyridinones

R	$\Delta \log D$	$\Delta \log D$	$\Delta \log D$	$\Delta \log D$
Me	0.63	0.24	0.48	
Et	0.33	0.68	0.49	
Pr	0.52	0.48	0.49	
Bu				0.53
pentyl				0.66
hexyl				

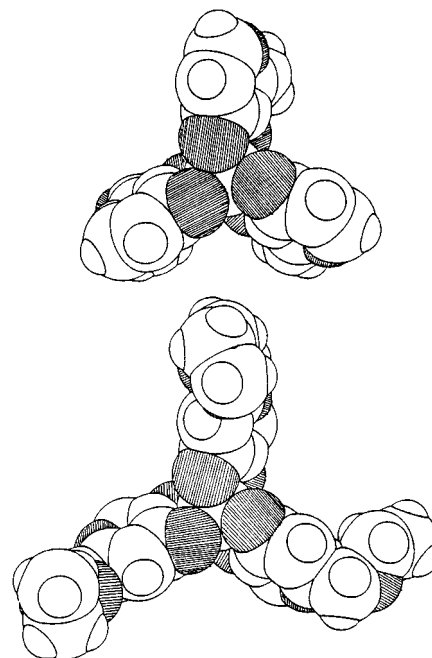


Figure 9. Space-filling drawings of indium complexes **37** and **38**.

The indium complexes (**37** and **38**) of representatives from both classes of compound namely **7** and **14**, respectively, were subjected to X-ray diffraction analysis (Figures 5 and 6). As expected, the complex containing the longer side arms (**38**) provides a much larger surface area for solvation by the organic phase than does the smaller complex of **37** (Figure 9). The contrast between the values of the D complex/ D free ligand ratios is probably further enhanced by the position of substitution of the alkyl chain. Thus the majority of the compounds with the high ratios have substituents which are not adjacent to the chelating portion of the ligand. In contrast all the compounds possessing low ratio values have the longest substituent adjacent to the coordination sphere of the metal. This difference could be related to the associated distortion of the octahedrally coordinated ion; there is a greater distortion in **37** than in **38**. Significantly compounds **12** and **31** fall at intermediate ratios with respect to the analogous compounds and consequently are located neither at the

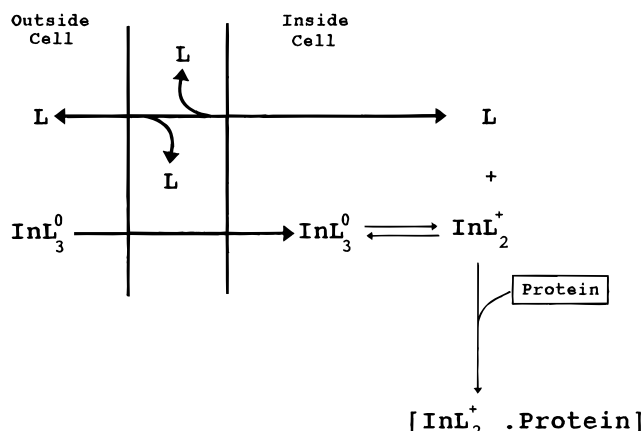


Figure 10. Transmembrane movement of both the indium complex and the free ligand leading to cell labeling by indium. The formation of the protein indium complex shifts the equilibrium thereby favoring accumulation of indium.

peaks or troughs of the relationship shown in Figure 3. The reason for the anomalous position of tropolone **2** is probably associated with its relatively low pK_a value. Thus, whereas all the other compounds in this study possess pK_a values > 8.5 , tropolone possesses a pK_a value of 6.7 and consequently is 83% dissociated at pH 7.4.

The selection of a suitable ligand for cell-labeling will be facilitated by the optimization of certain physical properties, thus to facilitate permeation of the cell membranes the $\log D$ value of the indium complex should be > 0 . However lipophilic chelators are potentially toxic^{38,39} and in order to minimize such toxicity the $\log D$ value of the free ligand should be limited to ≤ 1.0 . Many compounds investigated within this study fall within these two restrictions. The probable mechanism of cell-labeling by indium complexes is indicated in Figure 10. By virtue of the noncharged nature of the indium complex, the complex can enter the cell by simple diffusion. Inside the cell, the complex dissociates in the presence of proteins which are capable of providing alternative binding sites for indium. The resulting free ligand will leave the cell, again by simple diffusion. In principle, ligands which possess a high $\log D$ value for the complex (and thereby enhance the rate of cell entry) but a relatively low $\log D$ value for the free ligand (thereby minimizing potential toxicity associated with the ligand partitioning in the membrane phase (Figure 10)) should prove to be ideal for clinical use. Such compounds fall at the peaks of the $\log D$ complex/ $\log D$ free ligand curve (Figure 3). Significantly, tropolone, which is widely used for cell-labeling, is one such compound. Given the arbitrary cutoff values for toxicity of $\log D$ free ligand ≤ 1.0 , three other compounds are also identified as having a potential for cell-labeling, namely **13**, **14**, and **15**. Of this group the two more lipophilic compounds **14** and **15** were compared with tropolone in order to investigate their ability for cell-labeling.

The indium complexes of **14** and **15** label both red cells and leucocytes with a similar efficiency to that of tropolone (Figures 7 and 8). Indeed the labeling of "mixed" leucocytes with indium is marginally superior with both these novel ligands than that achieved using tropolone (Table 5). As 3-hydroxypyranones are relatively nontoxic compounds, this class of bidentate ligand

may offer advantages over the reagents currently used for cell-labeling with indium, namely tropolone and oxine. The relative molar concentrations of the 3-hydroxypyranones and tropolone ligands for cell-labeling were 1×10^{-3} and 4.4×10^{-3} M, respectively. The concentration of oxine in commercial preparations of ^{111}In -oxine is 3.45×10^{-4} M. Further cell labeling and toxicity investigations are currently in progress.

Experimental Section

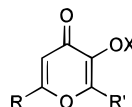
General Procedures. Melting points are uncorrected. IR spectra were recorded on a Perkin-Elmer 298. Proton NMR spectra were determined on a Perkin-Elmer R-32 (90 MHz). Mass spectra were obtained using Vacuum Generators 16 F (35 eV). Elemental analyses were performed by Butterworth Laboratories Limited, Teddington, Middlesex. Full spectroscopic and analytical data are available as supporting information.

Reagents. Benzyl chloride; boron tribromide, 1.0 M solution in dichloromethane; *N,N*-dimethylformamide, 99%; gallium atomic absorption standard solution (1000 $\mu\text{g}/\text{mL}$ of Ga in 1 wt % HNO_3); indium atomic absorption standard solution (1000 $\mu\text{g}/\text{mL}$ of In in 1 wt % HNO_3); iron(III) nitrate nonahydrate 99.99%; 1-methyl-2-pyrrolidinone 99%; MOPS, 99% (4-morpholinepropanesulfonic acid); 1-octanol, 99% HPLC grade; sodium hydride, 80% dispersion in mineral oil; zinc, dust 325 mesh (Aldrich Chemical Co., Dorset, UK). 2-(Hydroxymethyl)-5-hydroxy-4H-pyran-4-one 99% (kojic acid) (Janssen Chimica, Cheshire, UK). Acetaldehyde 99%; butyraldehyde, 99%; formaldehyde, 37 wt % solution in water; 1-iodobutane 99%; iodoethane 99%; iodomethane 99%; 1-iodopropane 99%; propionaldehyde, 97% (Fluka, Dorset, UK). 3-Methoxy-2(1H)-pyridone, 99% (Lancaster, Lancashire, UK). $^{59}\text{FeCl}_3$ in 0.1 M HCl (110–925 MBq/mg Fe) (Amersham Life Sciences, Buckinghamshire, UK). ^{67}Ga -citrate (carrier-free); $^{111}\text{InCl}_3$ in 0.04 M HCl (carrier-free) (Mallinckrodt Medical, Northampton, UK). Acid-citrate dextrose (NIH, formula A); phosphate buffered saline pH 7.4 (Pharmacy Manufacturing Department, Norfolk and Norwich Hospital, Norfolk, UK). Hespan (DuPont Pharma, Hertfordshire, UK). Tropolone, 0.054% w/v in HEPES-buffer pH 7.6 (Pharmacy Manufacturing Department, Ipswich Hospital, Ipswich, UK).

3-(Benzyloxy)-4H-pyran-4-one (benzyl pyromeconic acid) (4). To a two-necked vessel fitted (250 mL) with a condenser were added benzyl comenic acid (10 g, 0.04 mol) and 1-methyl-2-pyrrolidinone (100 mL). The mixture was heated under reflux and stirred magnetically for 6 h. The solvent was removed azeotropically with *N,N*-dimethylformamide (100 mL) by high vacuum rotary evaporation. The resulting brown oil was extracted into dichloromethane and washed with 5% aqueous sodium hydroxide (3×100 mL). The organic layer was dried over anhydrous sodium sulfate, filtered, and concentrated to dryness. Recrystallization from toluene afforded colorless needles of benzyl pyromeconic acid **4** (4.1 g, 50%): mp 84–85 °C. ^1H NMR (DMSO- d_6) δ 8.35 (1H, s, 2-H), δ 8.18 (1H, d, 6-H) δ 7.45 (5H, s, benzyl CH), δ 4.45 (1H, d, 5-H), δ 5.0 (2H, s, benzyl CH_2); ν_{max} (Nujol) 1635 cm^{-1} .

3-Hydroxy-4H-pyran-4-one (pyromeconic acid) (5). To a round-bottomed flask (250 mL) equipped with a condenser and magnetic stirring bar were added benzyl pyromeconic acid **4** (5 g, 0.025 mol) and 4 M hydrochloric acid (50 mL). The mixture was gently heated under reflux for 1.5 h. The reaction mixture was then neutralized using 10 M sodium hydroxide and evaporated to dryness. Water (50 mL) was added to the residue, and the pH was adjusted to 11 by treatment with 10 M sodium hydroxide. The mixture was extracted with dichloromethane (3×50 mL). The pH of the aqueous layer was then adjusted to 3 using concentrated hydrochloric acid, and the product was extracted into dichloromethane (2×50 mL). The organic extracts were combined, dried over anhydrous sodium sulfate, filtered, and concentrated. Recrystallization from toluene afforded **5** as white needles (1.6 g, 57%): mp 113 °C. Anal. ($\text{C}_5\text{H}_4\text{O}_3$) C, H.

3-(Benzyloxy)-6-(methoxymethyl)-4H-pyran-4-one (8). To a three-necked round-bottomed flask (500 mL) fitted with

Table 7. Syntheses of 2,6-Alkyl-3-hydroxy-4H-pyran-4-ones


compd	R	R'	mp, °C	%yield	formula	anal.
5	H	H	113	57	C ₅ H ₄ O ₃	C, H
12	CH ₂ OMe	H	79–80	34	C ₇ H ₈ O ₄	C, H
13	CH ₂ OEt	H	73–74	46	C ₈ H ₁₀ O ₄	C, H
14	CH ₂ O <i>n</i> -Pr	H	63–64	67	C ₉ H ₁₂ O ₄	C, H
15	CH ₂ O <i>n</i> -Bu	H	34–35	30	C ₁₀ H ₁₄ O ₄	C, H
16	Me	H	153–155	62	C ₆ H ₆ O ₃	C, H
21	Me	Me	163–164	53	C ₇ H ₈ O ₃	C, H
22	Me	Et	107–108	45	C ₈ H ₁₀ O ₃	C, H
23	Me	<i>n</i> -Pr	129–130	50	C ₉ H ₁₂ O ₃	C, ^a H
24	Me	<i>n</i> -Bu	79–80	47	C ₁₀ H ₁₄ O ₃	C, ^b H

^a C: calcd, 64.27; found 63.63. ^b C: calcd, 65.92; found 65.41.

a pressure equalized dropping funnel and containing a magnetic stirring bar were added benzyl kojic acid (10 g, 0.043 mol) and dry *N,N*-dimethylformamide (200 mL). Iodomethane (14 mL, 0.215 mol) was added via the dropping funnel. The resulting light brown solution was stirred at 25 °C for 30 min. Sodium hydride (80% dispersion in mineral oil) (2.6 g, 0.086 mol) was placed in a three-necked round-bottomed flask (500 mL) and washed with hexane (3 × 10 mL) to remove the mineral oil. The flask was then equipped with a pressure-equalized dropping funnel (250 mL) and a condenser and then flushed with nitrogen. The light brown solution prepared above was added to the flask via the dropping funnel over a period of 1.5 h under nitrogen with vigorous stirring. During the addition the reaction mixture effervesced and became red. Toward the end of the addition the intensity of the red coloration diminished. The contents of the flask were stirred under nitrogen for a further 24 h. The reaction mixture was concentrated by high vacuum rotary evaporation, and the residue was dissolved in water (100 mL). The resulting solution was adjusted to pH 12 by treatment with 10 M sodium hydroxide and extracted with dichloromethane (3 × 200 mL). The organic extracts were combined, dried over anhydrous sodium sulfate, filtered, and evaporated to dryness. Recrystallization from ethanol afforded a white powder (5.8 g, 58%): m.p. 67–68 °C; ¹H NMR (DMSO-*d*₆) δ 8.20 (1H, s, 2-H), δ 7.40 (5H, s, benzyl CH), δ 6.40 (1H, s, 5-H), δ 4.95 (2H, s, benzyl CH₂), δ 4.28 (2H, s, CH₂O), δ 3.32 (3H, s, OCH₃); ν_{\max} (Nujol) 1630 cm⁻¹.

Analogous syntheses of benzyl kojic acid with ethyl iodide, propyl iodide, and butyl iodide gave the intermediates **9**, **10**, and **11**, respectively.

3-Hydroxy-6-(methoxymethyl)-4H-pyran-4-one (12). In a three-necked round-bottomed flask (500 mL) fitted with a condenser were placed **8** (8 g, 0.03 mol) and 4 M hydrochloric acid (150 mL). The mixture was refluxed for 2 h. After cooling, the reaction mixture was adjusted to pH 11 using 10 M sodium hydroxide and extracted with dichloromethane (2 × 50 mL). The aqueous layer was treated with concentrated hydrochloric acid to obtain pH 1 and extracted with dichloromethane (3 × 100 mL). The organic extracts were combined, dried over anhydrous sodium sulfate, filtered, and concentrated to dryness by rotary evaporation. Recrystallization from toluene afforded **12** white needles (1.7 g, 34%): mp 79–80 °C. Anal. (C₇H₈O₄) C, H.

Analogous reactions with **9**, **10**, and **11** gave compounds **13**, **14**, and **15** as shown in Table 7.

3-Hydroxy-6-methyl-4H-pyran-4-one (allomaltol) (16). To a three-necked round-bottomed flask (500 mL) equipped with a thermometer, pressure-equalized dropping funnel, condenser, and magnetic stirring bar were added chlorokojic acid (20 g, 0.125 mol) and water (150 mL). The mixture was stirred and heated to a temperature of 40 °C in an oil bath. Zinc dust (16.29 g, 0.25 mol) was added, and the reaction mixture was stirred vigorously at 60 °C. Concentrated hydrochloric acid (37 mL, 3 mol equiv) was added dropwise via the addition funnel over a period of about 1 h during which

the reaction mixture effervesced producing hydrogen. The slurry was left stirring for 2–3 h at 60 °C. The excess zinc was removed from the pale green reaction mixture by hot filtration. The filtrate was adjusted to pH 1 and extracted with dichloromethane (3 × 100 mL). The organic extracts were combined, dried over anhydrous sodium sulfate, filtered, and concentrated. Recrystallization from 2-propanol gave **16** as a white solid (9.8 g, 62%): mp 153–155 °C. Anal. (C₆H₆O₃) C, H.

2-(Hydroxymethyl)-3-hydroxy-6-methyl-4H-pyran-4-one (17). To a three-necked round-bottomed flask (250 mL) fitted with a pressure-equalized dropping funnel (50 mL) and containing a magnetic stirring bar were added **16** (9.4 g, 0.074 mol) and water (100 mL). The pH of the mixture was adjusted to 10.5 by treatment with 10 M sodium hydroxide. A solution of 37% aqueous formaldehyde (5.5 mL, 0.074 mol) was added slowly dropwise via the dropping funnel. The solution was left to stir at 25 °C for 24 h. The reaction mixture was acidified to pH 1 using concentrated hydrochloric acid, cooled, and allowed to crystallize. The product was removed by filtration to yield a yellow solid (10 g, 86%): mp 157–158 °C. ¹H NMR (DMSO-*d*₆) δ 8.8 (1H, sbr, OH), δ 6.2 (1H, s, 5-H), δ 5.7 (1H, sbr, CH₂OH), δ 4.4 (2H, d, CH₂OH), δ 2.3 (3H, s, CH₃); ν_{\max} (Nujol) 1660, 1610, 1580.

Analogous syntheses of **16** with acetaldehyde, propionaldehyde, butyraldehyde gave compounds **18**–**20**.

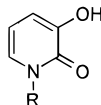
3-Hydroxy-6-methyl-2-propyl-4H-pyran-4-one (23). To a three-necked round-bottomed flask (500 mL) equipped with a thermometer, a pressure-equalized dropping funnel and containing a magnetic stirring bar were added **19** (7.9 g, 0.042 mol) and water (100 mL). Activated zinc dust (13.72 g, 0.21 mol) was added, and the mixture was stirred vigorously and heated to 60 °C in an oil bath. Concentrated hydrochloric acid (40 mL, 10 mol equiv) was added dropwise via the dropping funnel over a period of about 40–50 min during which the reaction mixture effervesced with the evolution of hydrogen. The mixture was stirred and heated at 60 °C for 24 h. The excess zinc was removed by filtration. The filtrate was adjusted to pH 1 and extracted with dichloromethane (3 × 100 mL). The organic layers were combined, dried over anhydrous sodium sulfate, filtered, and concentrated to dryness by rotary evaporation. Recrystallization from petroleum ether (60–80 °C) and toluene afforded a colorless solid **23** (3.5 g, 50%): mp 129–130 °C. Anal. (C₉H₁₂O₃) C, H.

Analogous reactions of **17**, **18**, and **20** gave compounds **21**, **22**, and **24**, respectively as shown in Table 7.

3-Methoxy-1-propyl-2H-pyridin-2-one (27). To a three-necked round-bottomed flask (500 mL) equipped with a pressure-equalized dropping funnel and a condenser carrying a calcium chloride drying tube were added 3-methoxy-2-(1*H*)-pyridone (2 g, 0.015 mol), potassium hydroxide (1.2 g, 0.022 mol), and 100 mL of dry propanol. Propyl iodide (3 mL, 0.03 mol) was added via the dropping funnel. The contents of the flask were concentrated by rotary evaporation, and the residue was extracted with dichloromethane (3 × 50 mL). The organic extracts were combined, washed with water (20 mL) and saturated sodium chloride solution (10 mL), dried over anhydrous sodium sulfate, filtered, and evaporated to dryness yielding a pale oil (2.5 g, 68%). ¹H NMR (DMSO-*d*₆) δ 7.30 (1H, d, 6-H), δ 6.85 (1H, d, 4-H), δ 6.20 (1H, t, 5-H), δ 3.94 (2H, t, NCH₂), δ 3.70 (3H, s, OCH₃), δ 1.75 (2H, m, CH₂CH₃), δ 0.91 (3H, t, CH₂CH₃).

Analogous reactions of 3-methoxy-2-(1*H*)-pyridone with methyl iodide, ethyl iodide, and butyl iodide in the corresponding dry alkanol gave intermediates **25**, **26**, and **27**.

3-Hydroxy-1-propyl-2H-pyridin-2-one (31). Compound **27** (2.5 g, 0.015 mol) was dissolved in dry dichloromethane (100 mL) in a three-necked round-bottomed flask (500 mL) fitted with a nitrogen inlet, bubbler and "Suba-Seal" pierced by a 4 in. 18 gauge needle and containing a magnetic stirring bar. The flask was flushed with nitrogen and then a small positive pressure of nitrogen maintained. The mixture was cooled to –70 °C by application of dry ice and acetone. A polypropylene syringe (50 mL) was charged with nitrogen and this was used to pressurize a Sure-Seal bottle containing a 1 M solution of boron tribromide in dichloromethane. Boron

Table 8. Syntheses of 1-Alkyl-3-hydroxy-2(1*H*)-pyridin-2-ones

compd	R	mp, °C	% yield	formula	anal.
29	Me	130–131	63	C ₆ H ₇ O ₂ N	C, H, N
30	Et	109–110	65	C ₇ H ₉ O ₂ N	C, ^a H, N
31	<i>n</i> -Pr	89–90	60	C ₈ H ₁₁ O ₂ N	C, H, N
32	<i>n</i> -But	60–61	70	C ₉ H ₁₃ O ₂ N	C, H, N

^a C: calcd, 60.42; found 59.82.

tribromide (15 mL, 1 mol equiv) was withdrawn from the bottle, and the syringe was detached and transferred to the needle on the reaction flask. After the addition, the solution was stirred under nitrogen. After 24 h, the flask was cooled to -70 °C and methanol (100 mL) was added dropwise. Nitrogen was passed through the system, water (2 × 50 mL) was added, and the mixture was concentrated to dryness by rotary evaporation. The residue was adjusted to pH 7, and the compound was extracted into dichloromethane (3 × 100 mL). The organic extracts were combined, dried over anhydrous sodium sulfate, filtered, and evaporated to dryness. Recrystallization from petroleum ether (100–120 °C) gave white needles (1.3 g, 60%); mp 89–90 °C. Anal. (C₈H₁₁O₂N): C, H, N.

Analogous reactions using **25**, **26**, and **28** gave compounds **29**, **30**, and **32**, respectively, as shown in Table 8.

Determination of Distribution Coefficients. Free Ligands (Method A). Distribution coefficients were determined using an automated continuous flow technique similar to that described by Tomlinson.²⁹ All distribution coefficient determinations were performed at 25 °C using AnalaR grade reagents under a nitrogen atmosphere. The aqueous and octanol phases were presaturated with respect to each other before use. The mixing chamber was a flat-based glass vessel (250 mL) equipped with a sealable lid. The filter probe consisted of a polytetrafluoroethylene plunger with a Blauband 589/3 cellulose filter paper (Schleicher and Schuell) which was wetted before being attached to the plunger by a net fastener to ensure the effective filtering of small droplets of octan-1-ol from the aqueous phase. The spectrophotometer (Pye-Unicam Lambda 5 UV/vis) and automatic dispenser (Metrohm 665 Dosimat) were interfaced with an OPUS II IBM compatible PC computer which controlled the system (using TOPCAT program)⁴⁰ as well as performing all calculations. A known volume (normally 40–100 mL) of MOPS buffer (50 mM pH 7.4, prepared using Milli-Q water) was placed in the flat-based glass mixing chamber. A peristaltic pump was used to circulate the buffer at a flow rate of 1 mL min⁻¹ through a spectrophotometer flow cell and back to the mixing chamber. Higher flow rates may introduce bubbles into the system which may induce a greater risk of droplets of hydrophobic phase being drawn into the probe. After a base line was obtained the solution was used for reference absorbance. A 1 × 10⁻⁴ M solution of the ligand was prepared in the aqueous phase (typically 40 mL) to give an absorbance of between 1.5 and 2.0 at the preselected wavelength. The computer program was initiated. When a constant absorbance was obtained (defined as an absorbance change of less than 0.002 absorbance units over a minimum of 100 individual readings) a suitable aliquot of octan-1-ol was added to the aqueous phase from the automatic dispenser. The two immiscible phases were continuously stirred to ensure effective partitioning of the sample compound. Subsequent absorbance readings were recorded until the system reached equilibrium when a further aliquot of octan-1-ol was added. The cycle was repeated for a series of additions of octan-1-ol. An estimate of the distribution coefficient was obtained from each octan-1-ol addition, which enabled calculation of a mean distribution coefficient value and standard deviation.

Iron Complexes (Spectroscopic Method). Distribution coefficients were determined using a 10:1 molar ratio of ligand to metal to ensure complete formation of the 3:1 neutral

complex. All distribution coefficient determinations were performed at 25 °C. The ligand was dissolved in 50 mL of MOPS buffer (20 mM pH 7.4, prepared using Milli-Q water and subsequently presaturated with octan-1-ol) to give a stock solution with a concentration of 1.1 × 10⁻³ M. Iron(III) nitrate nonahydrate was dissolved in 10 mL of 0.01 M HCl (prepared using Milli-Q water) at a concentration of 1 × 10⁻³ M. The iron(III) complexes were prepared by the addition of 9 mL ligand/buffer solution of 1 mL of the iron solution to give final concentrations of ligand and iron of 1 × 10⁻³ M and 1 × 10⁻⁴ M, respectively. The absorbance of the iron(III) complex solution was measured in the visible region between 300–900 nm using a Perkin-Elmer Lambda-5 Spectrophotometer. A 3 mL sample of the complex solution was equilibrated with 7 mL of octan-1-ol (presaturated with buffer) by shaking for 10 min. An aliquot of the aqueous layer was removed after centrifugation. The absorbance of the sample was measured following a further centrifugation to ensure that the sample was not contaminated with octan-1-ol. The distribution coefficient was calculated from the ratio of the equilibrium absorbance to the decrease in absorbance of the aqueous phase.

Metal Complexes (Method B). The ligand was dissolved in MOPS buffer (20 mM, pH 7.4, prepared using Milli-Q water and subsequently presaturated with octan-1-ol prior to use) to give a concentration of 1.1 × 10⁻³ M. For the metal solutions, iron(III) nitrate nonahydrate, gallium absorption standard solution (1010 μg of Ga per mL in 1 wt % HNO₃ ρ = 1.01 g cm⁻³), and indium absorption standard solution (990 μg of In per mL in 1 wt % HNO₃ ρ = 1.01 g cm⁻³) were prepared in 0.01 M HCl, respectively, each to a concentration of 1 × 10⁻³ M. To 2.5 mL of each solution were added 0.005–0.2 MBq of ⁵⁹Fe, ⁶⁷Ga, and ¹¹¹In to their respective solutions. Each solution was allowed to equilibrate. Solutions of the metal complexes were prepared by the addition of the ligand solution to each of the radiolabeled metal solutions. After equilibrium, 3 mL of the iron and gallium complex solutions and 5 mL of the indium complex solution was shaken with octan-1-ol (7 mL for iron and gallium complexes, 5 mL for indium complex) for 10 min. After centrifugation to separate the two immiscible phases, aliquots of each lower aqueous layer were removed and further centrifuged to remove any droplets of octan-1-ol. Aliquots of the partitioned metal complexes and of unpartitioned complexes were counted using a Compugamma γ counter. Distribution coefficients were calculated from the ratio of the counts per minute at equilibrium to the decrease in the counts per minute of the aqueous phase.

Metal Complexes (Method C). Ligands solutions were prepared similar to above except to concentrations of 1.1 × 10⁻⁴ or 1.1 × 10⁻⁵ M depending on the solubility. The metal solutions were prepared as above except to concentrations of 1 × 10⁻⁴ or 1 × 10⁻⁵ M. Solutions of the metal complexes were prepared by the addition of the ligand solution to the metal solution so that the concentration of ligand was 1 × 10⁻⁴ or 1 × 10⁻⁵ M and the metal 1 × 10⁻⁵ or 1 × 10⁻⁶ M ensuring that a ligand to metal ratio of 10:1 was maintained. The partitioning of the metal complexes was analogous to Method B except using 10 mL of aqueous phase and 100 μL of octan-1-ol.

X-ray Experimental. Compounds **37** and **38** were both crystallized from aqueous ethanol and methanol, respectively. Both the complexes formed colorless, platy crystals. The crystals of **37** were stable at room temperature, but those of **38** were unstable. All data were taken on an Enraf-Nonius CAD4 diffractometer. The intensity data of both the compounds were taken at low temperature. The crystal data, data collection parameters, and refinement results are summarized in Table 9. Both the structures were determined by the direct methods using the program SHELXS-86.⁴¹ The refinements were carried out by a full-matrix least squares routine using the program SHELX76⁴² for **37** and SHELXTL-plus⁴³ for **38**. The hydrogen atoms of **37** were located from the difference Fourier maps, and the hydrogen parameters were refined isotropically. In the last cycles of refinement, the positional coordinates of the five hydrogen of the ethyl group in **37** were not refined. For **38**, the hydrogen atoms were placed in their calculated positions and their contributions were included in the structure factor calculations, but the hydrogen parameters

Table 9. Crystal Data, Data Collection, and Refinement Parameters

	compound	
	37	38
formula	C ₂₁ H ₂₁ O ₉ In	C ₂₇ H ₃₃ O ₁₂ In
FW	532.0	664.4
crystal system	monoclinic	monoclinic
space group	P2 ₁ /n	C2/c
a	7.648(1) Å	28.500(6) Å
b	9.337(2)	15.545(3)
c	29.611(3)	13.212(3)
β	94.99(1)°	98.59(3)°
v	2106.6(6) Å ³	5788.0(10) Å ³
z	4	8
D _x	1.660 g/cm ³	1.525 g/cm ³
temperature	188 K	163 K
wavelength	0.71073 Å	0.71073 Å
radiation	Mo Kα	Mo Kα
crystal size	0.27 × 0.25 ± 0.03 mm	0.42 × 0.31 × 0.05 mm
F(000)	1080	2720
μ(Cu Kα)	0.81 mm ⁻¹	0.89 mm ⁻¹
2θ _{max}	53°	46°
diffractometer	CAD-4	Siemens P4
total unique reflections	4323	3756
no. of observed (I > 2σ(I))	2856	2637
absorption correction	integration	integration
max/min transmission	0.9531/0.8290	0.9659/0.8198
standard reflections	3, every 2 h	3, every 2 h
max variation	1.5%	5.5%
refinement	F	F ²
R	0.044	0.063
wR	0.042	0.151
no. of reflections	3119	2637
no. of variables	357	361
S	1.1	1.6
(Δ/σ) _{max}	0.02	0.07
Δρ(max) in diff map	0.63e/Å ³	1.0

were not refined. In **38**, the linear chains indicated some degree of disorder. The atoms C11, C12, and C13 in all three chains were subjected to restricted (keeping C–C distances within the range, 1.40–1.56 Å) refinement.

Biological Methods. The Effect of Ligand Concentration on Erythrocyte Uptake. The manipulation of human blood products was carried out using safe handling procedures. A 30 mL volume of fresh human venous blood was collected into a syringe containing 3 mL of ACD (formula A) with a 19 gauge needle. Whole blood was added to a 3 mL of Hespan (6% w/v hydroxyethyl starch in 0.9% sodium chloride) and allowed to stand for 45–60 min until erythrocyte sedimentation had occurred. Cell-free plasma was obtained by centrifugation of the supernatant. A 10 mL volume of packed erythrocytes were diluted with 5 mL of phosphate buffered saline (pH 7.4). Solutions of **14** and **15** were prepared in phosphate buffered saline at concentrations of 1×10^{-3} , 2×10^{-4} , 1×10^{-4} , and 1×10^{-6} M. The ¹¹¹In complexes were prepared by the addition of 1 mL aliquots of each ligand solution to 2 MBq of ¹¹¹InCl₃. The ¹¹¹In complexes were each incubated with an aliquot (1.75×10^9) of red cells (prepared by centrifugation of 300 μL of red cell suspension) at room temperature for 15 min. After incubation the cells were washed with cell-free plasma and the labeling efficiencies calculated by determining the ratio of the amount of activity on the cells to the amount of activity added to the cells.

Leucocyte Labeling and *in-Vitro* Plasma Stability Studies. Ligand solutions of **14** and **15** were prepared using phosphate-buffered saline (pH 7.4) at a concentration of 1×10^{-3} M. A 1 mL volume of the above solutions (1×10^{-3} M) and 1 mL of **2** (0.054% w/v prepared in HEPES–saline buffer pH 7.6) (4.4×10^{-3} M) was each added to 2 MBq of ¹¹¹InCl₃ (prepared in 0.04 M HCl). A 60 mL volume of whole blood (human) was collected by venupuncture into a 50 mL syringe containing 6 mL of ACD (formula A) with a 19 gauge needle. A 30 mL volume was transferred to each of two 50 mL Falcon tubes each containing 5 mL of Hespan. The tubes were

allowed to stand at room temperature for 45–60 min until erythrocyte sedimentation had occurred. The “mixed” leucocyte pellet was obtained by centrifugation of the leucocyte-rich–platelet-rich-plasma at 80 g for 10 min. Cell-free plasma was obtained by centrifugation of the resulting supernatant. The “mixed” leucocyte pellet was resuspended in cell free plasma to a total volume of 3.3 mL. A 800 μL volume of the cell suspension was transferred to three tubes and the three “mixed” leucocyte plugs each containing an identical number of cells ($3.3\text{--}5.5 \times 10^7$) were obtained by centrifugation. Each “mixed” leucocyte pellet was incubated with 1 mL of the ¹¹¹In complexes at room temperature for 15 min. After incubation the cells were washed with cell-free plasma and the labeling efficiencies calculated by determining the ratio of the amount of activity on the cells to the amount of activity added to the cells. The determination of *in-vitro* plasma stabilities were performed by the addition of 3 mL of cell-free plasma to each of the three cell aliquots and subsequent incubation at room temperature for 1 h. After centrifugation the supernatants were removed, and the activity was released from the cells was calculated. This process was repeated after 2, 3, and 4 h.

Acknowledgment. This research was supported by the British Technology Group, Cancer Research Campaign, and NIH (Project Grant: GM 21822). We wish to acknowledge assistance from Dr. Surinder S. Chana for the crystallization of indium(III) triethylmaltol and Dr. H. Khodr for help with speciation plots.

Supporting Information Available: Analytical data associated with hydroxypyranone and hydroxypyridinone synthesis and tables of X-ray final atomic positional coordinates, atomic thermal parameters, bond distances, and bond angles of **37** and **38** (20 pages). Ordering information is given on any current masthead page.

References

- Peters, A. M.; Saverymuttu, S. H. The value of indium-labeled leucocytes in clinical practice. *Blood Rev.* **1987**, *1*, 65–76.
- Thakur, M. L.; Segal, A. W.; Louis, L.; Welch, M. J.; Hopkins, J.; Peters, T. J. Indium-111-labeled cellular blood components: mechanism of labeling and intracellular location in human neutrophils. *J. Nucl. Med.* **1977**, *18*, 1020–1024.
- Thakur, M. L.; Lavender, J. P.; Arnot, R. N.; Silvester, D. J.; Segal, A. W. Indium-111-labeled autologous leukocytes in man. *J. Nucl. Med.* **1977**, *18*, 1012–1019.
- Dewanjee, M. K.; Rao, S. A.; Didsheim, P. Indium-111 tropolone, a new high-affinity platelet label: preparation and evaluation of labeling parameters. *J. Nucl. Med.* **1981**, *22*, 981–987.
- Danpure, H. J.; Osman, S.; Brady, F. The labeling of blood cells in plasma with ¹¹¹In. *Br. J. Radiol.* **1982**, *55*, 247–249.
- Danpure, H. J.; Osman, S. Optimum conditions for radiolabeling human granulocytes and mixed leucocytes with ¹¹¹In-tropolonate. *Eur. J. Nucl. Med.* **1988**, *13*, 537–542.
- Thakur, M. L.; Barry, M. J. Preparation and evaluation of a new indium-111 agent for efficient labeling of human platelets in plasma. *J. Labelled Compounds Radiopharm.* **1982**, *19*, 1410–1412.
- Thakur, M. L.; McKenney, S. L.; Park, C. H. Evaluation of indium-111-2-mercaptopyridine-N-oxide for labeling leukocytes in plasma: a kit preparation. *J. Nucl. Med.* **1985**, *26*, 518–523.
- Segal, A. W.; Deteix, P.; Garcia, R.; Tooth, P.; Zanneli, G. D.; Allison, A. C.; Indium-111 labeling of leucocytes: a detrimental effect on neutrophil and lymphocyte function and an improved method of cell labeling. *J. Nucl. Med.* **1978**, *19*, 1238–1244.
- Chisholm, P. M.; Danpure, H. J.; Healey, G.; Osman, S. Cell damage resulting from the labeling of rat lymphocytes and HeLa S3 cells with In-111 oxine. *J. Nucl. Med.* **1979**, *20*, 1308–1311.
- ten Berge, R. J. M.; Natarajan, A. T.; Hardeman, M. R.; van Royen, E. A.; Schellekens, P. T. Labeling with indium-111 has detrimental effects on human lymphocytes; concise communication. *J. Nucl. Med.* **1983**, *24*, 615–620.
- Kassis, A. I.; Adelstein, S. J. Chemotoxicity of indium-111 oxine in mammalian cells. *J. Nucl. Med.* **1985**, *26*, 187–190.
- Hider, R. C.; Hall, A. D. Clinically useful chelators of trispositive elements. In: *Progress in Medicinal Chemistry*; Ellis, G. P., West, G. B., Eds.; Elsevier: New York, 1991; Vol. 28, pp 41–173.
- Finnegan, M. M.; Lutz, T. G.; Nelson, W. O.; Smith, A.; Orvig, C. Neutral water-soluble post-transition-metal chelate complexes of medical interest: aluminium and gallium tris(3-hydroxy-4-pyridonates). *Inorg. Chem.* **1987**, *26*, 2171–2176.

- (15) Matsuba, A.; Nelson, W. O.; Rettig, S. J.; Orvig, C. Neutral water-soluble indium complexes of 3-hydroxy-4-pyrones and 3-hydroxy-4-pyridinones. *Inorg. Chem.* **1988**, *27*, 3935–3939.
- (16) Clevett, D. J.; Lyster, D. M.; Nelson, W. O.; Rihela, T.; Webb, G. A.; Orvig, C. Solution chemistry of gallium and indium 3-hydroxy-4-pyridinone complexes in vitro and in vivo. *Inorg. Chem.* **1990**, *29*, 667–672.
- (17) Porter, J. B.; Huehns, E. R.; Hider, R. C. The development of iron chelating drugs. In *Ballière's Clinical Haematology*; Hershko, C., Ed.; Ballière Tindall: London, 1989; Vol. 2, pp 257–292.
- (18) Gralla, E. J.; Stebbins, R. B.; Coleman, G. L.; Delahunt, C. S. Toxicity studies with ethyl maltol. *Toxicol. Appl. Pharmacol.* **1969**, *15*, 604–613.
- (19) Rennhard, H. H. The metabolism of ethyl maltol in the dog. *J. Agric. Food Chem.* **1971**, *19*, 152–154.
- (20) Singh, S.; Epemolu, R. O.; Dobbin, P. S.; Tilbrook, G. S.; Ellis, B. L.; Damani, L. A.; Hider, R. C. Urinary metabolic profiles in human and rat of 1,2-dimethyl- and 1,2-diethyl-substituted 3-hydroxypyridin-4-ones. *Drug Metab. Dispos.* **1992**, *20*, 256–261.
- (21) Tate, B. E.; Miller, R. L. Preparation of gamma-pyrones US Patent 3130204, 1964.
- (22) Bowden, K.; Heibron, I. M.; Jones, E. R. H.; Weedon, B. C. L. Researches on Acetylenic compounds. Part 1. The preparation of acetylenic ketones by oxidation of acetylenic carbinols and glycols. *J. Chem. Soc.* **1946**, 39–45.
- (23) Hare, L. E.; Lu, M. C.; Sullivan, C. B.; Sullivan, P. T.; Counsell, R. E. Aromatic amino acid hydroxylase inhibitors. 3. In vitro inhibition by azadopamine analogs. *J. Med. Chem.* **1974**, *17*, 1–5.
- (24) Campbell, K. N.; Ackermann, J. F.; Campbell, B. K. Studies on γ -pyrones. I. Derivatives of kojic acid. *J. Org. Chem.* **1950**, *15*, 221–226.
- (25) Rogers, E. F.; Dybas, R. A.; Hannah, J. Anticoccidial complexes. US Patent 3926935, 1975.
- (26) McOrmie, J. F. W.; Watts, M. L.; West, D. E. Demethylation of aryl methyl ethers by boron tribromide. *Tetrahedron* **1968**, *24*, 2289–2292.
- (27) Harris, W. R.; Carrano, C. J.; Cooper, S. R.; Sofen, S. R.; Avdeef, A. E.; McArdle, J. V.; Raymond, K. N. Co-ordination chemistry of microbial iron transport compounds. 19. Stability constants and electrochemical behavior of ferric enterobactin and model complexes. *J. Am. Chem. Soc.* **1979**, *101*, 6097–6104.
- (28) Dobbin, P. S.; Hider, R. C.; Hall, A. D.; Taylor, P. D.; Sarpong, P.; Porter, J. B.; Xiao, G.; van der Helm, D. Synthesis, physicochemical properties and biological evaluation of N-substituted 2-alkyl-3-hydroxy-4(1H)-pyridinones: Orally active iron chelators with clinical potential. *J. Med. Chem.* **1993**, *36*, 2448–2458.
- (29) Tomlinson, E. Filter-probe extractor: a tool for the rapid determination of oil-water partition coefficients. *J. Pharm. Sci.* **1982**, *71*, 602–604.
- (30) Cantwell, F. F.; Mohammed, H. Y. Photometric acid-base titrations in the presence of an immiscible solvent. *Anal. Chem.* **1979**, *51*, 218–223.
- (31) Fujita, T.; Iwasa, J.; Hansch, C. A substituent constant, π , derived from partition coefficients. *J. Am. Chem. Soc.* **1964**, *86*, 5175–5180.
- (32) Matsuba, C. A.; Nelson, W. O.; Rettig, J.; Orvig, C. Neutral Water-Soluble Indium complexes of 3-Hydroxy-4-pyrones and 3-Hydroxy-4-pyridinones. *Inorg. Chem.* **1988**, *27*, 3935–3939.
- (33) Matsuba, C. A.; Rettig, S. J.; Orvig, C. Main group (IIIA) complexes of benzohydroxamic acid and the crystal structure of tris(benzohydroxamato)indium(III). *Can. J. Chem.* **1988**, *66*, 1809–1811.
- (34) Finnegan, M. M.; Rettig, S. J.; Orvig, C. A Neutral Water-Soluble Aluminium Complex of Neurological Interest. *J. Am. Chem. Soc.* **1986**, 5033–5035.
- (35) Brown, S. D.; Burgess, J.; Fawcett, J.; Parsons, S. A.; Russell, Waltham, E. Three Polymorphic Forms of 2-Ethyl-3-hydroxy-4-pyranone- (Ethyl Maltol). *Acta Crystallogr.* **1995**, *C51*, 1335–1338.
- (36) Hider et al. (1995), unpublished results.
- (37) Tute, M. S. Principles and practice of Hansch Analysis: A guide to structure-activity correlation for the medicinal chemist. In *Advances in Drug Research*; Harper, N. J., Simmonds, A. B., Eds.; Academic Press: London, 1971; Vol. 6, pp 1–77.
- (38) Albert, A.; Hampton, A.; Selbie, F. R. The influence of chemical constitution on anti-bacterial activity. Part VII: The site of action of 8-hydroxyquinoline (oxine). *Br. J. Exp. Pathol.* **1954**, *35*, 75–84.
- (39) Albert, A.; Rees, C. W.; Tomlinson, A. J. H.; Why are some metal-binding substances anti-bacterial? *Recueil* **1956**, *75*, 819–824.
- (40) Hall, A. D. TOPCAT Program for Determination of Distribution Coefficients, King's College, University of London, 1990.
- (41) Sheldrick, G. M. SHELX76, Program for the Solution of Crystal Structure, University of Cambridge, England, 1984.
- (42) Sheldrick, G. M. SHELX-86. Program for the solution of Crystal Structures, University of Gottingen, Germany, 1986.
- (43) Sheldrick, G. M. SHELXTL-plus. Siemens Analytical X-ray Instruments Inc., Madison, WI, 1993.

JM960220G